An Experimental Study on the Impact of Wormlike Micellar Droplets onto Solid Surfaces

Hossein Baghlani, Mahmood Norouzi, Mohammad Hassan Kayhani, Mojtaba Ghatee, Mirae Kim, and Kyung Chun Kim

Abstract The present study investigates the impact of wormlike micellar droplets on dry solid horizontal surfaces experimentally. Here, the wormlike micellar sample is an aqueous solution of Cetyltrimethylammonium bromide (CTAB) and Potassium bromide (KBr). The effects of impact speed, surface roughness, and the viscosity and elasticity of the liquid phase on the spreading and receding of the droplet are studied in detail. The droplets are formed via 14G and 16G needles and the speed of impact is in the range of 2–3 m/s. The solid surfaces are plates of plexiglass and stainless steel. The results are compared with the impact of equivalent Newtonian droplets to investigate the effect of rheological properties. It is found that fluid elasticity causes a decrease in the spreading and an increase in the receding of droplets. The stress analysis suggests that this normal force is primarily a result of elongational viscosity, while the influence of the first normal stress difference on these dynamics is minimal.

Keywords Wormlike Micelle · Droplet impact · Solid surface

1 Introduction

The impact of droplets on solid surfaces has some important applications in painting, inkjet printing, spray coating, cleaning, cooling, pesticide deposition, and so on. The former studies in this field are mostly restricted to Newtonian cases and few reports are available in the literature for different classes of non-Newtonian fluids. German and Bertola [1] studied the effect of shear-thinning viscosity and yield stress on the

H. Baghlani · M. Norouzi (✉) · M. H. Kayhani
Faculty of Mechanical Engineering, Shahrood University of Technology, Shahrood, Iran
e-mail: mnorouzi@shahroodut.ac.ir

M. Ghatee
Faculty of Materials Science and Engineering, Shahrood University of Technology, Shahrood, Iran

M. Kim · K. C. Kim
School of Mechanical Engineering, Eco-friendly Smart Ship Parts Technology Innovation Center, Pusan National University, Busan 46241, Republic of Korea

D. Kim et al. (eds.), *Fluid-Structure-Sound Interactions and Control*, Lecture Notes in Mechanical Engineering, https://doi.org/10.1007/978-981-97-6211-8_33

impact of non-Newtonian drops on solid surfaces. They found that the morphology of shear-thinning drops is similar to the Newtonian cases while central drop peaks occur at the end of the inertial spreading of viscoplastic liquids. Mondani et al. [2] investigated the impact of Boger liquids on solid surfaces experimentally. They reported that the receding velocity is increased by increasing the impact velocity on hydrophilic substrates. Norouzi et al. [3] studied the same problem for the impact of Boger liquid on inclined dry surfaces. Based on their results, the effects of impact velocity and fluid viscosity on spreading and receding velocities decrease at the back of the impact point by reducing the drop impact angle.

The wormlike micellar solutions (WMS) are a class of non-Newtonian liquids from the molecular structure point of view. They are the flexible aggregation of surfactant amphiphilic lipid molecules and show some special rheological behavior such as shear-banding in the steady shearing test and single-mode Maxwell response in the sweep frequency test. There is a dearth in the literature on the impact of WMS drops on solid surfaces. In the present work, we tackle this problem empirically. The effects of impact speed, surface roughness, and the viscosity and elasticity of the liquid phase on the spreading and receding of the droplet are studied in detail.

2 Materials and Methods

The used wormlike micellar sample is an aqueous solution of Cetyltrimethylammonium bromide (CTAB) and Potassium bromide (KBr). To prepare the samples, at first, 3.64 g CTAB is dissolved in 100cc triple distilled water via a magnetic hotplate stirrer at 30C for 8 h. Then, we should wait for 3 h to obtain a homogenized and clear solution. Finally, 1.18 g KBr is dissolved via stirrer at 30C for 8 h. The rheological data of samples have been measured via an Anton-Paar MCR-302 rheometer utilizing a parallel plate measuring system with a diameter of 27 mm at 25C. A test was carried out to assess the sweep amplitude at a consistent low frequency of 1 Hz in order to determine the extent of the linear viscoelastic response. The storage and loss moduli remained stable even when subjected to strains of up to 40%. Consequently, the frequency sweep was conducted at a 10% strain level to ensure the generation of a linear dataset. The data of steady shear and oscillatory tests are depicted in Fig. 1. In the case of wormlike micellar solutions, they exhibit a response consistent with the single model Maxwell response during the frequency sweep test:

$$G' = \frac{\eta\omega^2}{1 + \lambda^2\omega^2}, \tag{1}$$

$$G'' = \eta_s\omega + \frac{\eta\omega}{1 + \lambda^2\omega^2}. \tag{2}$$

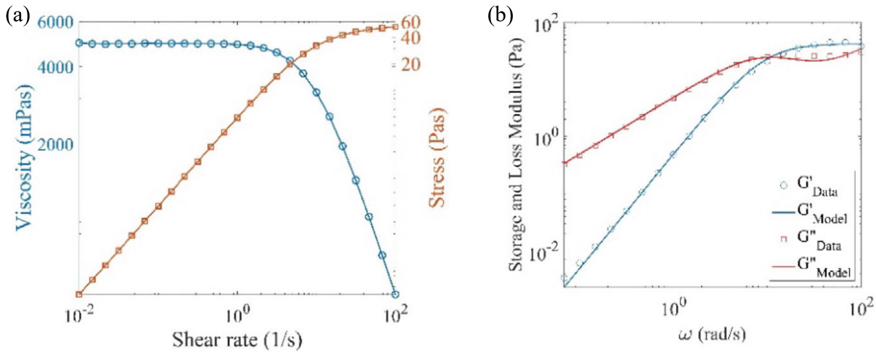

Fig. 1 Rheological data of WLM at 25C, **a** viscosity and shear stress and **b** storage and loss modulus

where G' is storage modulus, G'' is loss modulus η_s is the viscosity of a Newtonian solvent, ω is the frequency, and λ are the viscosity and the relaxation time. The error function, f, between the output of the model and the experimental data is defined as:

$$f = \sum_{j=1}^{m}\left[\left(1 - \frac{G'_{Model}(\omega_j)}{G'_{Data}(\omega_j)}\right)^2 + \left(1 - \frac{G''_{Model}(\omega_j)}{G''_{Data}(\omega_j)}\right)^2\right]. \quad (3)$$

where m is the number of data points. A hybrid genetic algorithm was used to minimize the error function. As a result, the relaxation time of the sample is equivalent to the reciprocal of the frequency at the point of crossover. In Fig. 1b, the response of the single-mode Maxwell model on the frequency sweep test is shown. According to the figure, the fitness between the model and rheological data is suitable which indicates the formation of WLMs.

The first normal stress difference is also assessed measured during steady shear test. The Ψ_1 value decreases with a power-law index of 0.4 within the power-law region. Since there is no experimental apparatus available for measuring the extensional viscosity (η_E) of dilute polymeric solutions in our lab, this property is approximated using a viscoelastic model. We used the Giesekus model to estimate this property. The reliability of the Giesekus model in estimating the extensional viscosity of viscoelastic fluids has been corroborated in the works of James [4]. Nonetheless, it should be noted that calculating η_E through any viscoelastic model is inherently an approximate prediction. The constitutive equation for this model is as follows:

$$\boldsymbol{\tau} = \boldsymbol{\tau}_p + \boldsymbol{\tau}_s \quad (4)$$

$$\boldsymbol{\tau}_p + \lambda d(\boldsymbol{\tau}_p) + \frac{\alpha\lambda}{\eta_{p0}}(\boldsymbol{\tau}_p \cdot \boldsymbol{\tau}_p) = 2\eta_{p0}\boldsymbol{D} \quad (5)$$

$$\boldsymbol{\tau}_s = 2\eta_s\boldsymbol{D} \quad (6)$$

In this context, the stress within a viscoelastic solution, denoted as $\boldsymbol{\tau}$, is determined as the combination of the stress from the Newtonian solvent, $\boldsymbol{\tau_s}$, and the contribution from the polymeric additives, $\boldsymbol{\tau_p}$. In Eq. (5), the variables are defined as follows: λ represents the relaxation time, D signifies the deformation tensor, η_s corresponds to the viscosity of the Newtonian solvent, and $\eta_{p,0}$ denotes the viscosity of the polymeric additives under zero shear rate conditions.

Furthermore, the parameter α pertains to the mobility factor, and its origin can be attributed to factors like anisotropic Brownian motion and/or anisotropic hydrodynamic drag acting upon the constituent polymer molecules. This term governs the extent of the shear-thinning behavior exhibited by the model, with typical values falling within the range of 0–0.5 for the majority of polymeric solutions and melts. Additionally, the term $d(\tau_p)$ represents the upper convective derivative of the polymeric stress, as defined as [5]:

$$d(\boldsymbol{\tau}_p) = \left(\frac{\partial}{\partial t} + \boldsymbol{u} \cdot \nabla\right)\boldsymbol{\tau}_p - \left((\nabla \boldsymbol{u}^T)\boldsymbol{\tau}_p + \boldsymbol{\tau}_p(\nabla \boldsymbol{u})\right) \tag{7}$$

In the context of steady uniaxial elongational flow with a non-zero α, the behavior of the Giesekus model is described as follows:

$$\frac{\eta_E}{3\eta_0} = \frac{\xi}{\lambda} + \left(1 - \frac{\xi}{\lambda}\right)\frac{1}{6\alpha} \times \left[3 + \frac{1}{\lambda\dot{\varepsilon}}\left\{\sqrt{1 - 4(1 - 2\alpha)\lambda\dot{\varepsilon} + 4\lambda^2\dot{\varepsilon}^2} + \sqrt{1 + 2(1 - 2\alpha)\lambda\dot{\varepsilon} + \lambda^2\dot{\varepsilon}^2}\right\}\right] \tag{8}$$

where $\dot{\varepsilon}$ is the strain rate. The above formulation is used to estimate the elongational viscosity.

The surface tension was measured utilizing a pendant droplet measurement device, which also has the capability to measure the contact angle (as a Goniometer). The solid surfaces are the stainless steel and Plexiglas. Surface roughness was quantified using the Intra Touch Method (ITM), employing the Marwin XP 20 apparatus fitted with the LP C 10-20-25/12 1103 probe. The measured average surface roughness, denoted as Ra, was found to be 0.20 µm for stainless steel and 0.84 µm for the Plexiglas material in use. Surface roughness plays a pivotal role in shaping the behavior of droplets when they collide with solid surfaces. This fact has led to the focused examination of how surface roughness impacts the dynamics of droplet impacts in various studies. In the current research, we aim to investigate how droplets' rheological properties affect their behavior upon impact. As a result, our findings are constrained to surfaces possessing the specified level of roughness. The exploration of how roughness and sharp edges affect the impact of viscoelastic droplets is a proposed avenue for future research endeavors. The drops are formed by samples' injection with a syringe pump from 14 and 16G needles. The drop impact is visualized via high-speed imaging (via Pco.dimax S1 camera) and its deformation is measured

Table 1 Physical properties of the used fluids

Physical property	WLM	Glycerol-water (57%/43%)	Glycerol-water (69%/31%)	Glycerol-water (78%/22%)	Glycerol-water (89%/11%)
Surface Tension (N/m)	66.7	66	64	64	63
Density (kg/m^3)	1065	1194	1201	1227	1236
Viscosity (mPa s)	Shear-Thinning	57	69	78	89

by image processing. The equivalent diameter of droplets is also calculated from the following relationship:

$$D = \sqrt[3]{d_v d_h^2} \tag{9}$$

We have taken into account two different impact velocities and two distinct needle sizes, resulting in a total of four distinct impact scenarios for Wormlike Micellar (WLM) drops. The viscosity of WLMs is contingent on the shear rate, leading to four distinct effective viscosities during the impact. To address this variability, we employed four equivalent Newtonian samples in our research, which consist of water and glycerol mixtures. By comparing the impact of WLM droplets with that of equivalent Newtonian fluids, we can investigate the influence of fluid elasticity. The properties of the used fluids including the surface tension coefficient, density and viscosity are mentioned in Table 1. For the sake of simplicity, throughout the rest of the paper, we will refer to any equivalent Newtonian fluids by mentioning only the concentration of glycerol.

3 Results and Discussion

Figure 2a, b illustrate the expansion length (L) of WLM and WG-57% droplets as they impact the Plexiglas surface at varying velocities. Both types of droplets were generated using a 16G needle, resulting in equivalent diameters of 3.01 mm for WLM and 3.16 mm for WG-57%, respectively. As the impact velocity increases, the expansion length (L) also increases for both types of droplets. However, it's noteworthy that the positive effect of the velocity increase on the expansion length (L) is more pronounced for the Newtonian fluid than for the WLM. Figure 3 provides a more detailed visualization of this effect. In Fig. 3a, b, the parameter L is presented for two impact scenarios involving both WLM and equivalent Newtonian samples. It is evident that both the spreading and receding of WLM droplets are less pronounced compared to the equivalent Newtonian samples.

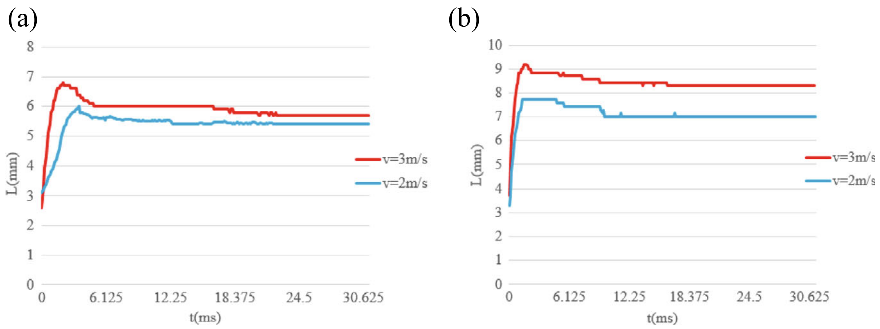

Fig. 2 The expansion length of drop versus time, **a** impact of WLM droplet formed via 16G needle on to Plexiglas surface and **b** impact of WG-57% droplet formed via 16G needle on to Plexiglas surface

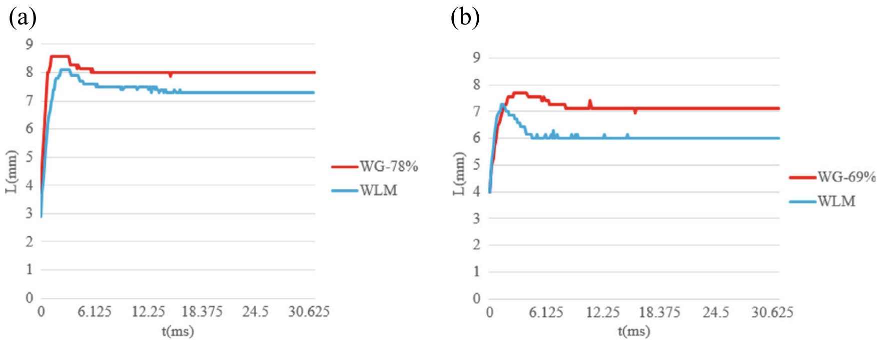

Fig. 3 The expansion length of drop versus time, **a** impact of droplets formed via 16G needle at v = 3m/s and **b** impact of droplets formed via 14G needle at v = 2m/s

As indicated in Table 1, the surface tension coefficients of the samples exhibit a notable degree of similarity. Consequently, the variation in expansion length between WLM and the Newtonian fluids can be attributed to the normal forces in WLM sample. The impact of a droplet onto a solid surface can be viewed as a combination of shear and elongational flow. In the case of WLM samples, this impact generates a normal force, which is the result of both the first normal stress difference and the elongational viscosity. The first normal stress difference arises as large molecules align along the streamlines during shear deformation, while elongational viscosity originates from the resistance of polymeric molecules during stretching. In Fig. 4a, we observe the ratio of the total normal stress to the shear stress during the spreading of WLM on the Plexiglass surface in the course of the impact process. As depicted in the figure, there is a substantial normal force opposing the droplet's spreading. Figure 4b presents the ratio of the normal stress stemming from elongational flow to the first normal stress difference. It is evident from this graph that the contribution of elongational viscosity to the total normal force far outweighs the impact of the first normal stress difference. Consequently, it can be inferred that the limited expansion of WLM droplets compared to equivalent Newtonian droplets can be attributed to the pronounced elongational viscosity exhibited by WLM samples.

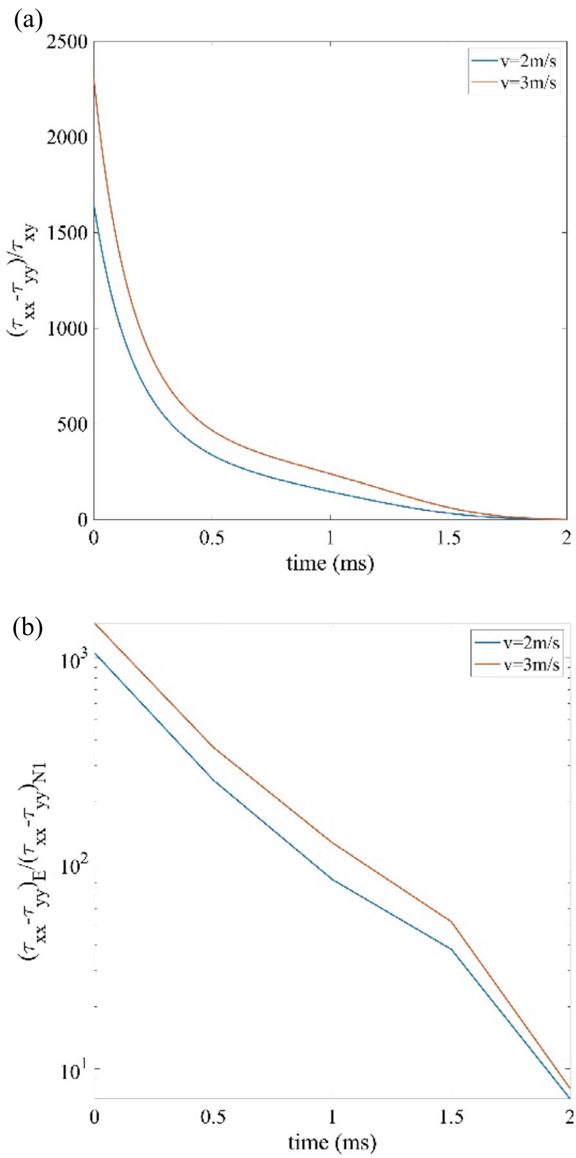

Fig. 4 The normal stress ratios during the spreading of WLM droplet, **a** ratio of total normal stress to the shear stress and **b** the ratio of normal stress arising from elongational viscosity to the first normal stress difference

4 Conclusions

To summarize, we carried out experimental research on the impact behavior of droplets, both Newtonian and WLM, when they collide with flat surfaces. We observed that higher impact velocities resulted in greater droplet extension. When we compared these findings with those of equivalent Newtonian fluids, we noted that Newtonian fluids displayed more extensive spreading and retraction compared to WLMs. The normal force within WLM droplets played a constraining role, limiting both the spreading and receding of the droplets. Our stress analysis suggests that this normal force is primarily a result of elongational viscosity, while the influence of the first normal stress difference on these dynamics is minimal.

Acknowledgements This work was supported by Brain Pool Program through the National Research Foundation of Korea (NRF) funded by the Ministry of Science and ICT (NRF-2022H1D3A2A01091637). This work was also supported by the National Research Foundation of Korea (NRF) grant, which is funded by the Korean government (MSIT) (No. 2020R1A5A8018822, No. 2021R1C1C2009287).

References

1. German G, Bertola V (2009) Impact of shear-thinning and yield-stress drops on solid substrates. J Phys Condens Matter 21:1–16
2. Mandani S, Norouzi M, Shahmardan MM (2018) An experimental investigation on impact process of Boger drops onto solid surfaces. Korea-Austr Rheol J 30(2):99–108
3. Norouzi M, Sheykhian MK, Shahmardan MM, Shahbani-Zahiri A (2021) Experimental investigation of spreading and receding behaviors of Newtonian and viscoelastic droplet impacts on inclined dry surfaces. Meccanica 56:125–145
4. James DF (2009) Boger fluids. Annu Rev Fluid Mech 14:129–142
5. Bird RB, Armstrong RC, Hassager O (1987) Dynamics of polymeric liquids, vol 1: fluid mechanics, 2nd edn. Wiley, New York